Multiple temperature sensors embedded in an ultrasonic "spiral-like" waveguide

Cite as: AIP Advances **7**, 035201 (2017); https://doi.org/10.1063/1.4977965
Submitted: 18 August 2016 . Accepted: 21 February 2017 . Published Online: 01 March 2017

Suresh Periyannan, Prabhu Rajagopal, and Krishnan Balasubramaniam

Multiple temperature sensors embedded in an ultrasonic "spiral-like" waveguide

Suresh Periyannan, Prabhu Rajagopal, and Krishnan Balasubramaniam[a]
Centre for Non Destructive Evaluation and Department of Mechanical Engineering, Indian Institute of Technology Madras, Chennai, Tamil Nadu 600 036, India

(Received 18 August 2016; accepted 21 February 2017; published online 1 March 2017)

This paper studies the propagation of ultrasound in spiral waveguides, towards distributed temperature measurements on a plane. Finite Element (FE) approach was used for understanding the velocity behaviour and consequently designing the spiral waveguide. Temperature measurements were experimentally carried out on planar surface inside a hot chamber. Transduction was performed using a piezo-electric crystal that is attached to one end of the waveguide. Lower order axisymmetric guided ultrasonic modes L(0,1) and T(0,1) were employed. Notches were introduced along the waveguide to obtain ultrasonic wave reflections. Time of fight (TOF) differences between the pre-defined reflectors (notches) located on the waveguides were used to infer local temperatures. The ultrasonic temperature measurements were compared with commercially available thermocouples. [http://dx.doi.org/10.1063/1.4977965]

I. INTRODUCTION

Ultrasonic temperature sensors are of much interest for temperature profile measurement requirements in several industrial applications (e.g., power plants). While thermocouples and resistive temperature devices (RTD) are commonly used in current industrial temperature sensing, they suffer from sensor drift during long term operation.[1] The footprint of a thermocouple, involving two wires and often ceramic coatings/beads, flexibility of these wires, their ability to measure temperature only in one location and failure of hot junction at high temperature are limiting factors for industrial applications. The ultrasonic waveguide technique has the potential to address some of these limitations. Efforts on the measurement of physical properties surrounding fluids (such as molten glass, mould powder slags, viscous fluids, etc.) and temperature dependent elastic moduli of the waveguides surrounded by air using waveguide approaches have been reported.[2–11] An ultrasonic system has been developed for air temperature measurement using phase shift records.[12,13] A Lithium-Niobate crystal[14] and surface acoustic waves[15] were shown to improve surface temperature measurements. Temperature distribution in a solid was measured using phase shift of acoustic beam.[16] Most of the previous approaches described measurements limited to a single zone of interest. Using these approaches, it would be necessary to have multiple sensors for multi-point distributed measurements. Our group has demonstrated multi-point measurements over a linear region. In the present paper, a novel single ultrasonic waveguide in a spiral configuration is shown to yield the possibility for multiple distributed sensing on a plane. This approach has some similarities to reports in the literature on distributed fiber optic temperature sensors using Fiber Bragg Grating reflectors[17,18] using a light source along with wavelength division multiplexing. In our approach (see Refs. 2, 19, and 20 for detailed descriptions), the ultrasonic reflected signal and the time of flight differences are employed for measurement of local temperatures. Waveguide sensor approaches for distributed temperature and environmental measurements have been presented by the authors, especially using a helical embodiment.[19,20]

[a]Email: balas@iitm.ac.in for the corresponding author, Telephone : 044-22575688.

The work here focuses on the spiral-like (pan-cake) configuration of the waveguide and uses pairs of notch reflectors to localize the measurement gage lengths in a planar surface. The main (and perhaps only) similarity between the spiral and the helical[19] configurations is that both propose the use of time of flight measurement from ultrasonic wave reflections from notches in a single waveguide for temperature measurement at multiple locations. In comparison, the spiral configurations provide a 2-dimensional (planar) or even in some instances a 3-dimension (volumetric) distributed temperature measurement. Also, the spiral waveguide here does not have the phenomena of the "twist" in the cross-section of the waveguide and hence allows for the use of both thin and/or thick waveguides. Finally, in comparison to spring-like helical waveguides, the wave dispersion effect in spiral configuration is not as much of an issue as long as the minimum diameter is larger than twice the wavelength (this is discussed later in section III). For this, Finite Element (FE) simulations were employed to better understand the physics of ultrasonic guided waves in spiral configurations and to select the appropriate spiral dimensions.

II. BACKGROUND

A. Waveguide temperature sensors

The measurement of the relative time of flight (TOF) between these reflections (notches) can be monitored and used to obtain the temperature between the two reflectors (for more details on waveguide sensors[19,20]). Here, each pair of reflections can be considered as one sensor to determine the temperature of the surrounding medium; the physical distance between these reflectors is the gage length.

In Figure 1(a–c), the waveguide of interest is illustrated in three possible spiral configurations. Figure 1(a) illustrates a spiral waveguide that allows for realizing different mean diameter values by adjustment of the radial pitch between two successive coils. Figure 1(b) presents a form of circular waveguide with single mean diameter, to cover large region of interest in a plane. Figure 1(c) again

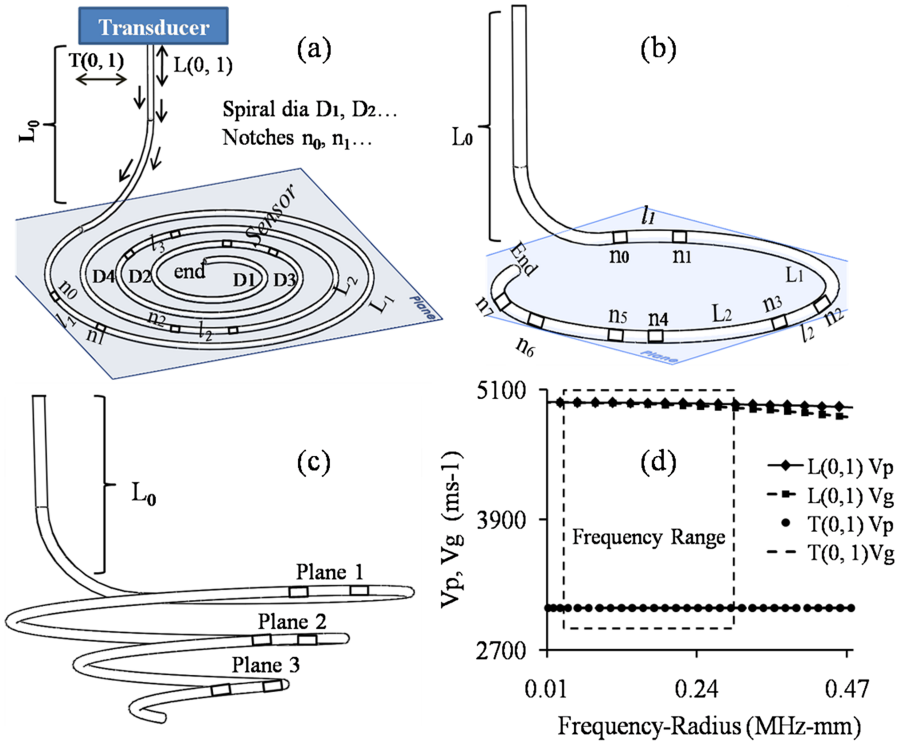

FIG. 1. Illustration of temperature measurement concept in (a, b, c) spiral, circular and conical waveguides respectively, (d) dispersion plot for a straight Chromel wire.

presents a conical spring waveguide that can be pulled in the axial direction, allowing for sensors to be placed at different planes at various depths.

Also, it may be possible to measure the different depths of temperature in a hot chamber by rotating the spiral or circular waveguide from, for example, 0° to a 90° plane. The compressed position in Figure 1(a) allows for temperature measurements in one plane that are relatively closely spaced, compared to the waveguides shown in Figure 1(b–c). The spiral waveguide can be easily re-configured in radial and axial directions (1D, 2D, 3D) based on the measurement region of interest.

The design of the spiral waveguide can be modified by, (a) increasing or decreasing the number of active coils, (b) adjusting the mean diameter (radial pitch) (c) pulling the spiral waveguide axial direction. In this paper, notch type of embodiments (approximately 0.5 mm deep and 3 mm long) were machined along the length of the 1.18 mm diameter waveguide to provide reflected signals from each sensor embodiment.

B. Ultrasonic waves in spiral wire waveguide

Three families of wave modes are considered: longitudinal (L), torsional (T) and flexural (F) that propagate in the axial direction (z) of the cylindrical coordinate system (r, θ and z).[21] The frequency range, phase velocity (V_p) and group velocity (V_g) chosen are based on the non-dispersive region of interest in the corresponding straight wire waveguide of same radius, using DISPERSE[22] as shown in Figure 1(d). The dispersion effects observed are due to (a) the diameter of the waveguide, (b) the frequency of operation, and (c) the curvature effects of the spiral, and must be considered while designing the waveguide sensor.

The fundamental longitudinal L(0,1) is first used to understand guided wave behaviour in a spiral waveguide. Subsequently, both L(0,1) and fundamental torsional T(0,1) modes are considered for experimentally demonstrating the distributed measurement of temperature. The T(0,1) mode is non-dispersive (due to the effects (a) and (b), that is, for straight waveguides) over the entire range of frequencies. In comparison, the L(0,1) mode is non-dispersive only in the low-frequency regime. Hence, an operational frequency range of 200 - 500 kHz was chosen for the experiments. In order to ensure low dispersion, an appropriate thickness of the wire and suitable mean diameter (spiral diameter) were selected using FE simulations as described in the next section.

Studies of waves in curved waveguides were reported in literature in the context of acoustic waves, electromagnetic waves[23,24] and elastic waves[25,26] with applications in civil structures. The dispersion effects due to the curvature of a helical structure (Chromel wire) were studied at different mean diameters.[19] The dispersion effects of longitudinal and torsional waves were considered and analyzed for cylindrical and helix geometries using a finite element approach in a non-orthonormal coordinate system.[25] The study shows that by increasing the helix radius, the helix effect on wave propagation and the dispersion caused by curvature can be significantly reduced. The previously reported literature on spiral-like waveguides are limited to optical/microwave domain and have been used for applications such as devising a delay/filter circuit, design of antennas or electro-mechanical speakers.[27–30] We have sought to extend similar concepts for distributed temperature measurements using ultrasonic guided waves.

III. SPIRAL WAVEGUIDE DESIGN USING FINITE ELEMENT (FE) SIMULATION

The dispersion effect due to curvature was studied for a spiral configuration of Chromel wire having circular cross-section, using FE models, as shown in Figure 2(a, b). For elastic moduli of the material, a typical Chromel wire waveguide in a straight configuration was employed and the group velocities V_g were experimentally obtained as, V_g for L(0,1) = 4983 m/s and V_g for T(0,1) = 3082 m/s at room temperature using previously reported approache.[31]

Wave propagation simulation studies, using elasto-dynamic FE models implemented in ABAQUS® (http://www.3ds.com/) have been earlier reported for helical spring-like and bent waveguides.[19,31,32] Similar wave propagation simulations (pulse-echo mode) were performed on the spiral waveguide. The parameters used in the FE models are listed in Table I (based on mesh refinement and computational stability[19,25,31–33]). Temperature effects were not considered in our studies.

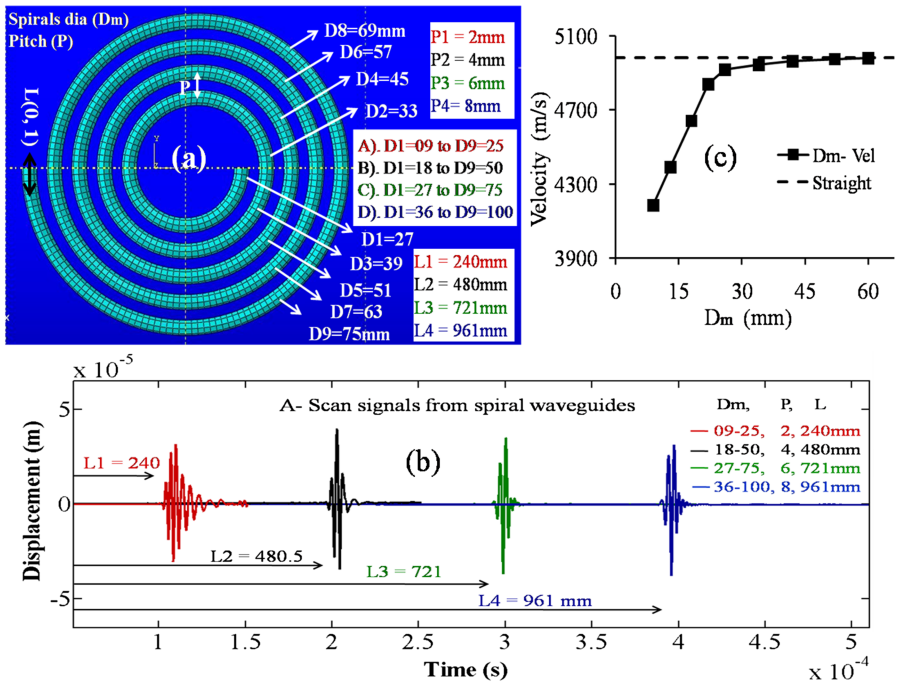

FIG. 2. (a) Spiral waveguide dimensions at different parameters, (b) A-Scan of the far end reflected signals obtained in pulse echo mode at different D, P and L values, and (c) V_g vs. D_m of spiral waveguide.

The axial input excitation used to generate Longitudinal L(0,1) mode was given at one end of the spiral waveguide as shown in Figure 2(a), in the form of a three (n=3) cycle Hanning windowed toneburst displacement centered at required frequency. A-scan signals were obtained at the same excitation nodes by plotting the displacements as function of time. The mean diameter, length and radial pitch of spiral waveguide (without notches for all Cases A-D are shown in Figure 2(a–b)) can be measured using Equations (1–3) for this FE simulation, where λ is the wavelength of the longitudinal wave.

$$\text{Mean diameter of the spiral waveguide } (D_m) = b\lambda;\ (b = 0.54 \text{ to } 6.02) \tag{1}$$

$$\text{Length of the wires (L1, L2, L3, L4 for Case A-D)} = \pi/2 \sum_1^m D_m \quad m = 1,\ 2,.. \tag{2}$$

$$\text{L1 or L2 or L3 . . .} = (\pi/2)\,(D_1 + D_2 + D_3 + \ldots) \text{ where } D_m \text{ varies} \tag{2a}$$

$$\text{Radial pitch of the spiral waveguide (P)} = \frac{D_{m+2} - D_m}{2} \tag{3}$$

The longitudinal L(0,1) mode A-Scan signals represent the free far end reflections in spiral waveguides without any embodiments (notches) using pulse-echo mode. Each A-scan was observed from different parameters of the spiral waveguides by varying D_m as shown in Figure 2(b). Significant

TABLE I. Material properties and spiral waveguide parameters for FE simulation studies.

Material	Mass Density-ρ (Kg m^{-3})	Young's Modulus-E (GPa)	Poisson Ratio-μ	Element Size & Type	L, d in (mm)	Spirals (D) in (mm)	Pitch (p) mm	No of cycle(n), Freq(f) (Hz)
Chromel	8650	214.8	0.30	λ/34, 8-node Brick	240-961, 1.18	0.54 λ to 6.02 λ	2, 4, 6, 8	3, 300e3

TABLE II. The V_g obtained using FE simulation for different spiral parameters.

Case	D1-Dm, P, L,	Dimensions (mm)	No of spiral	Vg (m/s)
A	D1-D9, P1, L1	9-25, 2, 240	9	4678
B	D1-D9, P2, L2	18-50, 4, 480	9	4868
C	D1-D9, P3, L3	27-75, 6, 721	9	4932
D	D1-D9, P4, L4	36-100, 8, 961	9	4972

changes were observed in L(0,1) mode group velocity (V_g) due to changes in mean diameters of the spiral waveguide (D1-D9, P1, L1 to D1-D9, P4, L4 in Table II). The signal was observed to be relatively dispersive in nature, when the D_m (see Case A: 9, 11, 13, 15 mm) is $< \lambda$. When the range of the spiral diameters was increased from 9-25 mm to 36-100 mm in Cases A-D, the signal obtained was relatively dispersion-free and the velocity increased by 294 m/s. The individual velocity of each mean diameter ($D_m < \lambda$ to $D_m > \lambda$) of waveguide was measured using FE models as shown in Figure 2(c). Due to the curvature effect, the velocity decreased, somewhat linearly with D_m for mean diameters $< 2\lambda$.

In a helical waveguide, the pitch is dependent on the mean diameter and helix angle. However in a spiral waveguide, the change in pitch is dependent on the change in two successive mean diameters. Here, the change in velocity was due to the curvature effects ($D_m < \lambda$). Similar velocity changes and dispersion issues were observed by varying the helix angle (pitch) and mean coil diameter (curvature effect) in a helical waveguide in earlier reports.[19,25,26] It is observed that the wave propagation behavior is significantly influenced by the selection of the mean diameter of spirals which are based on the wavelength (λ). Therefore, mean diameters $>2\lambda$ were chosen for the design of the spiral waveguide to reduce the dispersion effect. The observations from the FE results are summarized as follows:

a) The dispersive nature of wave propagation in a spiral waveguide embodiment is dependent on wire thickness, mean diameter and excitation frequency, as expected.
b) The modes were dispersive when the mean diameter (D_m) was $< \lambda$, and in this region, the group velocity reduces as D_m decreases.
c) For $D_m > 2\lambda$ the wave modes were found to be non-dispersive and propagate with a group velocity V_g close to that for a straight wire waveguide.

IV. RESULTS AND DISCUSSION

A. Experimental apparatus description

Figure 3(a) shows the spiral waveguide used in the experiment to measure temperature in a high temperature test furnace. Details of the experimental setup and procedure has been described elsewhere by the authors.[2,11,19,20,34] Multiple notches were machined along the length of the Chromel spiral waveguide as shown in Figure 3(a, b). The notches were positioned in order to avoid the overlapping of reflected signals from each notch as shown in Figure 3(c).

Ultrasonic PZT Transducer (Panametrics NDT V151, 500 kHz broadband) and data acquisition system (NI USB-5133) were used to acquire and archive the A-scan signals (pulse echo) of waveguide from the pulser-receiver (Panametrics 5077PR) to a computer. Multiple reflected signals from multiple pair notches were continuously monitored using the signal peak-tracking technique. Subsequently, the change in time of flight (δTOF) between each pair of notches (one sensor) were calculated using Equation (4). The TOF's and the δTOF's of multiple sensors in the waveguide were recorded at different temperatures inside the furnace.

Instantaneous time of flight difference (δTOF) of a waveguide is defined as shown below.

$$(\delta TOF_{n+1})_i = [TOF_{(n+1)i} - TOF_{ni}] - [TOF_{(n+1)} - TOF_n] \quad (4)$$

where, TOF_{ni}, TOF_n Instantaneous (i) TOF at various temperature and (ii) TOF at room temperature from each notch location n $(\delta TOF_{n+1})_i$ Instantaneous change in TOF between the reflections from each sensor location n, in μs.

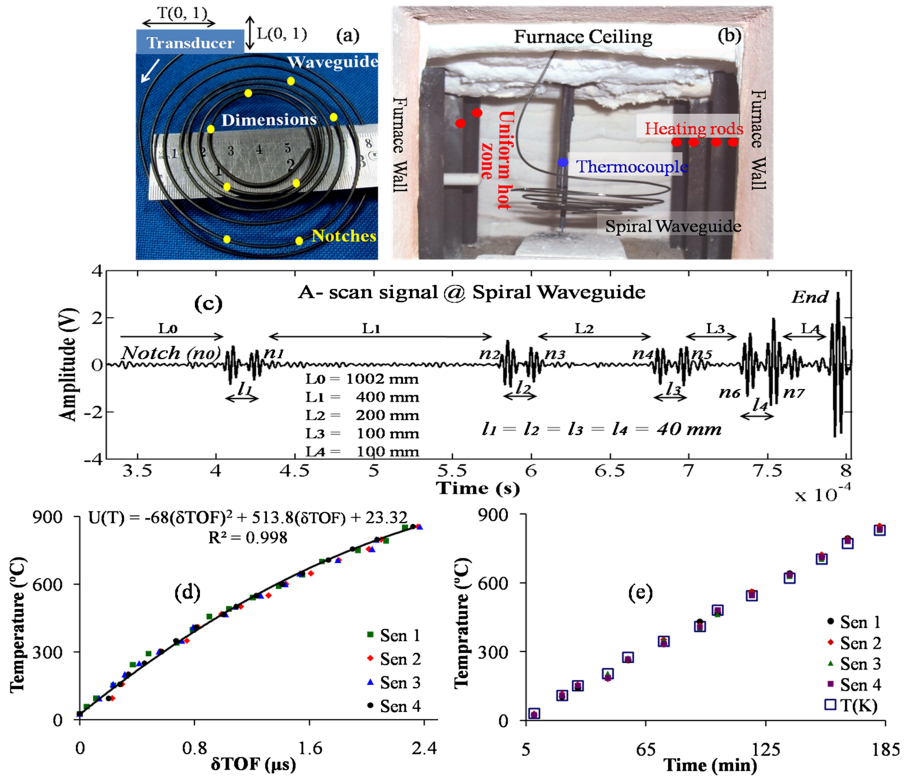

FIG. 3. (a) Photograph of Chromel spiral waveguide with notches, (b) Experimental setup of spiral waveguide system with melter, (c) Reflected signals from the four pair of notches and the end of the spiral waveguide, (d). δTOF vs. Temperature for spiral waveguide sensor representing the calibration curve, (e) Comparison of temperature measurement using ultrasonic waveguide method (solid) with thermocouple T(K) (hollow).

Each sensor's δTOF is measured in between the pair of notches ((0, 1), (2, 3), (4, 5), (6, 7)...) locations n at T_i

$$U(T) = -68(\delta TOF)^2 + 514(\delta TOF) + 23.3\,^{\circ}\text{Celsius} \tag{5}$$

B. Temperature measurement in a uniform hot region using L(0,1) mode

A spiral waveguide with four pair of notches and a furnace were used in this work as shown in Figures 3(a–b). The L(0,1) mode was generated/received in the spiral waveguide using the shear wave transducer procedure[11] and was oriented parallel (0°) to the axis of the waveguide. The instruments reported earlier were used to obtain the A-scan (Figure 3(c)) from the spiral waveguide with notches. The spiral waveguide was kept in the uniform hot region of the furnace as shown in Figure 3(b). Temperature was uniformly increased inside the furnace for about 3 hours to calibrate the waveguide sensor. A K-type thermocouple was co-located near the spiral waveguides and the corresponding temperature was monitored. The calibration was based on the time of flight difference (δTOF) at locations in-between the pair of notches (one sensor) using peak-tracking method that has been reported earlier.[19,20,34] The δTOF of each sensor was measured at instantaneous temperature using Equation (4). Spiral waveguide sensor number 4 was initially calibrated using with thermocouple output as shown in Figure 3(d). Equation (5) was found from the calibration plot using the 2nd order polynomial expression. Calibration of sensor number 4 was determined to be adequate for the other three sensors on the same waveguide. Each sensor TOF measurements were then related to the local temperature measurement using Equation (5). The thermocouple output was compared with the waveguide sensors output at different time instances as shown in Figure 3(e).

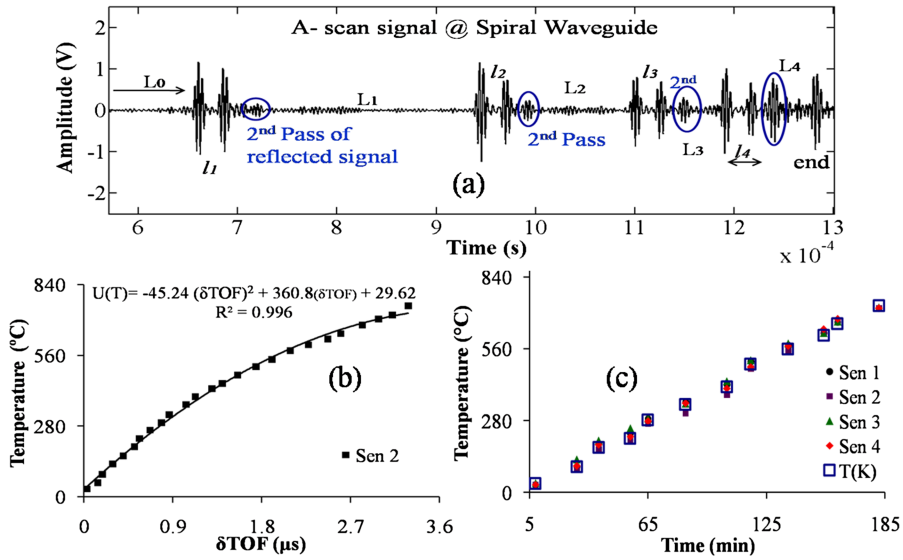

FIG. 4. (a) Shows the multiple reflected signals from the multiple pair of notches in a spiral waveguide b) Calibration curve, (c) Comparison of temperature measurement using ultrasonic waveguide with thermocouple T(K).

C. Temperature measurement in a uniform hot region using T(0,1) mode

The T(0,1) wave mode has a non-dispersive character at wide range of frequencies, compared to L(0,1) mode of the same material. The wavelength of the T(0,1) mode is significantly smaller compared to that of L(0,1) mode; thus the gage lengths (l_s) of the sensor and consequently the overall footprint of the spiral can be reduced. Sensitivity of this measurement is based on the effect of δTOF which depends on the type of wave mode. At 100 MHz digitization, the sensitivity of measurement was observed to be approximately 3.8° C for L(0,1) and 2.3° C for T(0,1) modes. Hence for the same gage length, T(0,1) is more sensitive. The T(0,1) mode transmission/reception procedure for spiral waveguide employed a shear wave crystal that was oriented 90° to the axis of the waveguide and has been reported in literature.[11]

$$U(T) = -45.2(\delta TOF)^2 + 361(\delta TOF) + 29.6\,^{\circ}\text{Celsius} \quad (6)$$

The A-scan signal obtained using shear wave transducer for spiral waveguide with notches is shown in Figure 4(a). In the A-scan signal, we were interested in the 1st pass of reflected signals from each pair of notches. The 2nd pass of reflected signals, including mode converted reflections, from each pair of notches are also marked in the A-scan plot. These signals were of relatively smaller amplitudes and if the spacing between the sensors are sufficiently large, these will not adversely influence the measurements. The waveguide sensors were calibrated using T(0,1) mode similar to the previous section. The change in time of flight (δTOF) of T(0,1) mode of the spiral waveguide sensor 2 was plotted with the thermocouple output as shown in Figure 4(b). Equation (6) was obtained from the calibration plot of sensor 2 and used for other sensors in the same waveguide. For each sensor, the temperature was calculated using Equation (6) and compared with the thermocouple's output at different time instances as shown in Figure 4(c).

V. SUMMARY AND CONCLUSION

This paper reported on the development of an ultrasonic spiral waveguide temperature sensor for a more robust, small footprint approach to distributed measurement of temperatures over a plane when compared to thermocouples or other waveguide methods. This technique uses several pairs of notches in a waveguide and each pair of notches was considered as one sensor. The spiral waveguide sensors using both guided L(0,1) and T(0,1) modes that can be generated and received by using

a shear transducer were demonstrated. 3D FE simulation was used to study the dispersion effects and to select suitable mean diameters (D_m) for the spiral waveguide design. The spiral waveguide sensor was calibrated based on the time of flight changes (δTOF) from L(0,1) and T(0,1) modes by uniformly varying the temperature inside the furnace. The calibration relationship for a particular mode is material dependent, provided D_m is above 2λ and hence must be performed only once for each material. Temperatures were measured and compared with thermocouple reading using both wave modes. The maximum temperature difference between the waveguide sensors and the thermocouple was observed to be less than 2%. In this work, only 4 pairs of notches were used in the spiral waveguide. It is possible to increase the number of sensors, but may depend on the material (Kanthal, Platinum, Tungsten, etc) and its ability to sustain the guided ultrasonic waves.

The T(0,1) mode has several advantages over L(0,1) mode,[20] however, the choice of the mode will depend on the specific measurement application. The mode-converted and multiple reverberations from the notch pairs were found to be relatively small and hence did not adversely affect the measurements. The signal strength from the notches located near the transducer is higher compared to the ones that were farther. These can be further reduced or even eliminated by more precise design of the notch type and dimensions. The position of the reflector locations, the D_m and the exact configuration of the spiral must be designed based on the measurement requirements as defined by the specific applications.

ACKNOWLEDGMENTS

The authors wish to thank the Board for Research in Nuclear Sciences (BRNS), Mumbai, INDIA, for financial support for this work.

[1] R. B. Bentley, Sensors and Actuators- A: Phy. **24**, 21 (1990).
[2] S. Periyannan and K. Balasubramaniam, Measurement **61**, 185 (2015).
[3] V. V. Shah and K. Balasubramaniam, Ultrasonics **34**(8), 817 (1996).
[4] R. Kazys, R. Sliteries, R. Raisuits, E. Zukaskas, A. Viladisauskas, and L. Meizka, App.Phy. Lett. **103**, 204102 (2013).
[5] K. Balasubramaniam, V. V. Shah, D. Costley, G. Bourdeaux, and J.P. Singh, Review of Scientific Instruments **70**(12), 1 (1999).
[6] K. Balasubramaniam, V. V. Shah, D. Costley, G. Bourdeaux and J. P. Singh, U.S. patent 6,296,385 (2 Oct 2001).
[7] V. V. Shah and K. Balasubramaniam, Ultrasonics **38**, 921 (2000).
[8] V.S.K. Prasad, K. Balasubramaniam, E. Kannan, and K.L. Geisinger, Journal of Materials Processing Technology **207**, 315 (2008).
[9] J.C. Pandey, M. Raj, S. N. Lenka, S. Periyannan, and K. Balasubramaniam, Journal of Iron Making and Steel Making **38**, 74 (2011).
[10] K. Balasubramaniam, S. Periyannan, U.S patent no. 20,16/0153,938 A1 (2 June 2016).
[11] S. Periyannan and K. Balasubramaniam, Review of Scientific Instruments **86**, 114903 (2015).
[12] K.N. Huang, C.F. Huang, Y.C. Li, and M.S. Young, IEEE, 294 (2003).
[13] W.Y. Tsai, H.C. Chen, and T.L. Liao, Sensors and Actuators- A: Phy. **132**, 526 (2006).
[14] A. Baba, C.T. Searfass, and B.R. Tittmann, App. Phy. Lett. **97**, 232901 (2010).
[15] R.G. Stearns, B.T.K. Yakub, and G.S. Kino, App. Phy. Lett. **43**, 748 (1983).
[16] D. Husson, S.D. Bennett, and G.S. Kino, App. Phy. Lett. **41**, 915 (1982).
[17] Y.J. Rao, Optics and Lasers in Engineering **31**(4), 297 (1999).
[18] K. Chen, X. Zhou, B. Yang, W. Peng, Q. Yu, Optics & Laser Technology **73**, 82 (2015).
[19] S. Periyannan, P. Rajagopal, and K. Balasubramaniam, J. App. Phy. **119**, 144502 (2016).
[20] S. Periyannan, P. Rajagopal, and K. Balasubramaniam, AIP Advances **6**, 065116 (2016).
[21] J.L. Rose, *Ultrasonic Waves in Solid Media* (Cambridge University Press, Cambridge, UK, 1999), pp. 143–152.
[22] B.N. Pavlakovic, M.J.S. Lowe, P. Cawley, and D.N. Alleyne, Review of Progress in Quantitative NDE **16**, 185 (1997).
[23] W. Sollfrey, J. App. Phy. **22**, 905 (1951).
[24] S. Ahn and A.K. Ganguly, IEEE Trans. on Electron Devices **33**(9), 1348 (1986).
[25] F. Treyssede, Wave Motion **45**, 457 (2008).
[26] F. Treyssede and L. Laguerre, Journal of Sound and Vibration **329**, 1702 (2010).
[27] A.D. Simard, Y. Painchaud, and S. LaRochelle, IEEE Photonics Society Annual Meeting 726 (2010).
[28] A.D. Simard, Y. Painchaud, and S. LaRochelle, Opt. Express **21**, 8953 (2013).
[29] Z. Chen, J. Flueckiger, X. Wang, H. Yun, Y. Wang, Z. Lu, F. Zhang, N. A. Jaeger, and L. Chrostowski, OSA Technical Digest (2015).
[30] G. Nichols, US Patent no 6,648,098 B2 (2003).
[31] S. Periyannan and K. Balasubramaniam, Experimental Mechanics **1** (2016).
[32] S. Periyannan, P. Rajagopal, and K. Balasubramaniam, Ultrasonics **74**, 211 (2017).
[33] P. Manogharan, X. Yu, Z. Fan, and P. Rajagopal, NDT & E International **75**, 39 (2015).
[34] S. Periyannan, P. Rajagopal, and K. Balasubramaniam, Physics Procedia **70**, 514 (2015).